

Pressure-induced structural transformations in the molybdate $\text{Sc}_2(\text{MoO}_4)_3$ W. Paraguassu,¹ M. Maczka,² A. G. Souza Filho,^{1,*} P. T. C. Freire,¹ J. Mendes Filho,¹ F. E. A. Melo,¹
L. Macalik,² L. Gerward,³ J. Staun Olsen,⁴ A. Waskowska,² and J. Hanuza^{2,5}¹*Departamento de Física, Universidade Federal do Ceará, P.O. Box 6030, Fortaleza-CE, 60455-900, Brazil*²*Institute For Low Temperature and Structure Research, Polish Academy of Science, P.O. Box 1410, 50950 Wrocław, Poland*³*Department of Physics, Technical University of Denmark, Building 307, DK-2800 Kgs. Lyngby, Denmark*⁴*Niels Bohr Institute, Oersted Laboratory, University of Copenhagen, Universitetsparken 5, DK-2100 Copenhagen, Denmark*⁵*Faculty of Industry and Economics, University of Economics, 118/120 Komandorska Str., 53-345 Wrocław, Poland*

(Received 10 June 2003; revised manuscript received 13 October 2003; published 16 March 2004)

High pressure Raman scattering and x-ray diffraction studies of the molybdate $\text{Sc}_2(\text{MoO}_4)_3$ are presented. A sequence of changing symmetry effects is observed through two structural phase transitions ending up with an amorphous state. The observed two structural phase transformations are reversible. The crystal to amorphous transition is irreversible. Our results point out that the amorphization process in $\text{Sc}_2(\text{MoO}_4)_3$ may be due to a kinetic hindrance of a phase transition rather than due to chemical decomposition effects as have been proposed to occur for some molybdates and tungstates.

DOI: 10.1103/PhysRevB.69.094111

PACS number(s): 62.50.+p

I. INTRODUCTION

The amorphization of crystals under high pressure conditions is a phase transition where the long range order symmetry breaks down. This phenomenon has been observed in several kinds of materials with all intermolecular bondings, such as van der Waals, covalent, ionic, metallic, and hydrogen bonds.¹ The reversibility of the crystal to an amorphous transition is one of the many intriguing issues behind the amorphization process. The reversible pressure-induced amorphization has been observed for a large number of materials²⁻⁶ for which the initial crystalline configuration is obtained when the pressure is released. The proposed mechanism responsible for the reversibility is based on the hypothesis that rigid polyatomic units remain intact through the crystal-amorphous transformation.⁶ An irreversible amorphization process has also been observed for a large number of materials¹ including tungstates⁷⁻¹⁴ and rare-earth molybdates $R_2(\text{MoO}_4)_3$ ($R = \text{Gd}, \text{Tb}, \text{Sm}, \text{Eu}$).^{15,16} This irreversibility has been attributed either to a mechanical deformation or the frustration of a phase transition (a kinetically impeded phenomenon),⁹ and to a chemical decomposition process.¹⁶

Among the materials for which the pressure-induced amorphization phenomenon has been observed, the molybdates and tungstates occupy a special place owing to their interesting physical-chemical properties, thereby making them good prototype materials to obtain new concepts about the physics of amorphization processes, about chemical decomposition,^{11,16} and about coordination changes¹³ under high pressure as well. In particular, the molybdate $\text{Sc}_2(\text{MoO}_4)_3$ is a special member of this family because it exhibits a negative thermal expansion (NTE) and a very flexible framework structure composed of corner-shared MoO_4^{2-} units.^{17,18} The NTE has been widely discussed in connection with the pressure induced amorphization process observed in some molybdates and tungstates.^{7-13,19} Perottoni and Jornada⁷ proposed that there is a close relationship between NTE and the pressure induced amorphization process in these flexible framework structures, i.e., both processes are

due to the instabilities of some low energy modes. Ravindran *et al.*⁹ suggested that amorphization has its origin either from a kinetic hindrance of an equilibrium phase transition or from a kinetic hindrance of equilibrium decomposition, thus suggesting that the linkage between NTE (related to structural instabilities) and amorphization (related to slow kinetic processes) is only marginal. As one can note, the amorphization phenomenon is a subject of intense debate, and still has several open issues to be addressed.

In this paper we study molybdate $\text{Sc}_2(\text{MoO}_4)_3$ single crystals under high pressure through Raman spectroscopy and x-ray diffraction. At about 0.29 and 2.7 GPa pressures, changes in the Raman spectra (softening and splitting of the stretching modes) indicated two crystal to crystal phase transitions. Upon increasing pressure the well defined Raman peaks start to get broaden with a dramatic decrease in intensity. These changes become dominant at about 4.0 GPa. The collapse of all the well resolved Raman peaks in broad bands at high pressures indicates a pressure-induced amorphization process in $\text{Sc}_2(\text{MoO}_4)_3$. The x-ray diffraction measurements confirms the presence of pressure induced amorphization. By releasing the pressure, we have observed that both crystal to crystal transitions in $\text{Sc}_2(\text{MoO}_4)_3$ are reversible processes. The crystal to amorphous transition is reversible if the applied pressure is below 5.1 GPa, but it becomes irreversible for higher pressures.

II. EXPERIMENT

Single crystals of $\text{Sc}_2(\text{MoO}_4)_3$ were grown by cooling the molten mixture containing $\text{Sc}_2(\text{MoO}_4)_3$ and solvent $\text{Na}_2\text{Mo}_2\text{O}_7$ in a 1:1 ratio. The cooling rate was 2 °C/h from 1020 to 840 °C and 5 °C/h down to room temperature. The pressure dependent Raman spectra were obtained with a triple-grating spectrometer (Jobin Yvon T64000) equipped with a N_2 -cooled charge coupled device (CCD) detection system. The line 488.0 nm of an argon ion laser was used as excitation. An Olympus microscope lens with a focal distance $f = 20.5$ mm and a numeric aperture of $\text{N.A.} = 0.35$ was

used to focus the laser beam on the sample surface. High-pressure Raman experiments were performed using a cryostat diamond anvil cell with a 4:1 methanol:ethanol mixture as the transmitting fluid. The spectrometer slits were set for a resolution of 2 cm^{-1} . In order to avoid any polarization effect to be observed in the spectra due to the eventual rotation of the sample inside the cell during pressure loading, we have used an optical device to destroy the polarization of both incident and scattered light.

High-pressure powder x-ray diffraction patterns were recorded at room temperature using the white-beam energy-dispersive method and synchrotron radiation at Station F3 of HASYLAB-DESY in Hamburg, Germany. High pressures were obtained in a Syassen-Holzapfel type diamond-anvil cell. A finely ground powder sample and a ruby chip were placed in a $200\text{-}\mu\text{m}$ -diameter hole of the inconel gasket, preindented to a thickness of $60 \mu\text{m}$. A 16:3:1 methanol:ethanol:water mixture was used as the pressure-transmitting medium. The Bragg angle was calculated from a zero-pressure diffraction spectrum of NaCl in the diamond-anvil cell. In the spectra shown, the lower level of the analog-to-digital converter has been set to cut off the Mo fluorescence lines. For both Raman spectroscopy and x-ray experiments the pressure calibration was achieved by using the well known pressure shift of the ruby luminescence lines.

III. RESULTS AND DISCUSSION

At room temperature and ambient pressure the $\text{Sc}_2(\text{MoO}_4)_3$ crystallizes in an orthorhombic structure (D_{2h}^{14} space group, $Z=4$) with 68 atoms per unit cell.^{17,18} A standard point group analysis leads to 204 degrees of freedom at the Brillouin zone center (Γ point) distributed among the irreducible representation of the D_{2h} point group as

$$\begin{aligned} \Gamma = & 25A_g + 26B_{1g} + 25B_{2g} + 26B_{3g} + 25A_u \\ & + 26B_{1u} + 25B_{2u} + 26B_{3u}. \end{aligned} \quad (1)$$

Selection rules state that only A_g , B_{1g} , B_{2g} , and B_{3g} are Raman active modes. The unpolarized Raman spectrum at room temperature and ambient pressure is shown in Fig. 1 (lower trace). The number of observed modes is much smaller than expected because the factor group splitting is too small to be resolved in the unpolarized spectra. Based on lattice dynamics calculations, polarized Raman scattering studies (not discussed in this paper),²⁰ and studies on an isomorphous material,²¹ we have identified the spectral ranges where we expect to observe the bending modes ($300\text{--}400 \text{ cm}^{-1}$), antisymmetric stretching modes ($810\text{--}960 \text{ cm}^{-1}$), and symmetric stretching modes ($960\text{--}990 \text{ cm}^{-1}$).

Provided these general aspects of the $\text{Sc}_2(\text{MoO}_4)_3$ at ambient conditions, we now move to analyze the pressure effects on the vibrational/structural properties of this crystal. Upon applying pressure, the Raman spectra exhibit changes at 0.29 GPa . We observe a splitting of the stretching modes very clear for the symmetric modes located in the $960\text{--}1000\text{-cm}^{-1}$ frequency range. For the antisymmetric stretching modes such a splitting is significantly smaller.

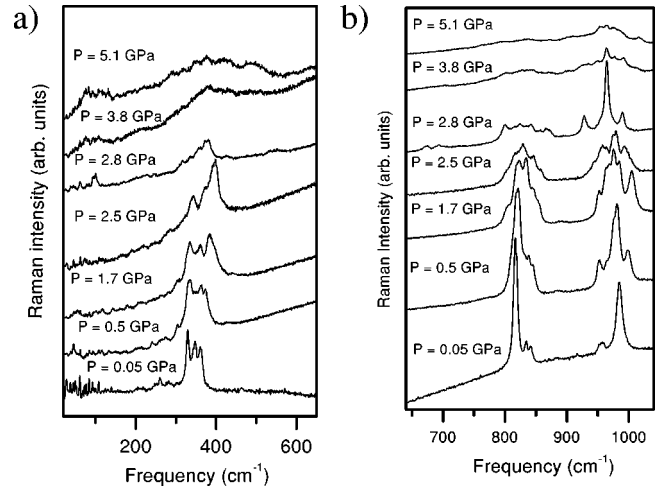


FIG. 1. Raman spectra of $\text{Sc}_2(\text{MoO}_4)_3$ crystals recorded at different pressures during compression experiments in the (a) low and (b) high frequency ranges.

This modification indicates the first structural phase transition in the compression run. More drastic changes occur at about 2.7 GPa . It is observed that some modes upshift or downshift during the compression along with changes in their relative intensity. The peaks at 330 , 347 , and 364 cm^{-1} , assigned to the bending modes of the MoO_4^{2-} tetrahedra, evolve to give rise to a broad band. The peak structures observed in the $810\text{--}850\text{-cm}^{-1}$, $950\text{--}960\text{-cm}^{-1}$, and $950\text{--}1000\text{-cm}^{-1}$ frequency ranges [see Fig. 1(b)] experience drastic changes as can be observed in the spectrum recorded at 2.8 GPa pressure. The observed changes indicate a second structural phase transition whereby the structure of the new phase differs significantly from the structures of the two stable phases below 2.7 GPa .

By further increasing pressure new and remarkable changes in the Raman spectra are observed. At around 3.7 GPa , the higher frequency stretching modes start to lose their sharpness (linewidths of $\sim 5 \text{ cm}^{-1}$) and all of them develop an excessive broadening, thus resulting in a broad band (linewidth of $\sim 50 \text{ cm}^{-1}$) centered at about 970 cm^{-1} . This anomalous broadening points out to a breakdown in the translational symmetry of the system, thus suggesting that the $\text{Sc}_2(\text{MoO}_4)_3$ experienced a gradual transition from an ordered to a disordered state between 3.7 and 5.1 GPa , i.e., pressure has induced an amorphization process. The main changes observed in the spectra can be followed by analyzing the frequency ω vs pressure P plot shown in Fig. 2. The results shown in Fig. 2 clearly indicate that the material experiences structural modifications at about $P=0.29$, 2.6 , and 3.7 GPa . All the peaks can be well fit with a linear pressure dependence $\omega(P) = \omega_0 + \alpha P$. It is noticeable that some modes present negative α values that are typically observed in materials that exhibit the NTE phenomenon.^{7,12}

In order to get more insight into the behavior of $\text{Sc}_2(\text{MoO}_4)_3$ under pressure, we have performed additional x-ray studies (see Fig. 3). These studies show very clearly significant changes in the diffraction pattern of the sample measured at ambient [Fig. 3(a)] and 4.0 GPa [Fig. 3(b)] pressures, indicative of the 2.7 GPa phase transition. The x-ray

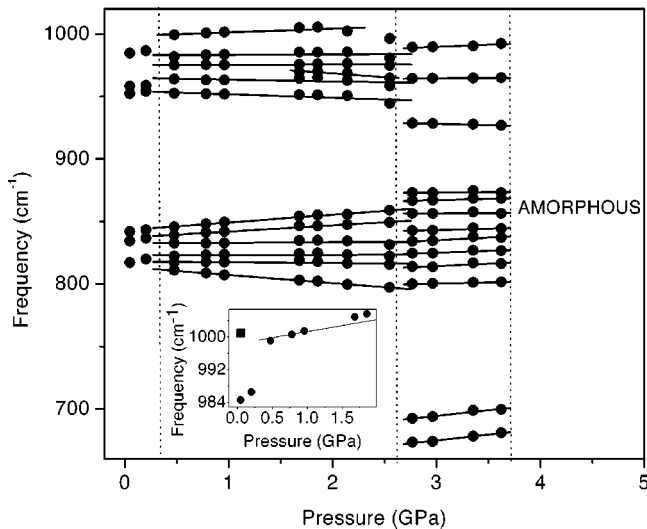


FIG. 2. Frequency vs pressure plot of the stretching modes observed in $\text{Sc}_2(\text{MoO}_4)_3$ crystals for compression experiments. The solid lines are linear fits on the data to $\omega(P) = \omega_0 + \alpha P$. The solid square in the inset stands for the frequency of the stretching modes observed in the low temperature phase (Ref. 20).

data also show that as a result of pressure the diffraction peaks starts to broaden and a very broad background appears in the pattern obtained at $P = 6.0$ GPa [see Fig. 3(c)]. These changes clearly reveal that the gradual amorphization of the sample starts slightly below 4.0 GPa.

The observed phase transitions in $\text{Sc}_2(\text{MoO}_4)_3$ is the first definitive proof of a pressure induced phase transition in any member of the orthorhombic or closely related monoclinic $M_2(\text{XO}_4)_3$ compounds ($M = \text{Sc, Al, In, Fe, Cr; X} = \text{Mo, W}$).^{17,22} The first phase transition occurs at about 0.29 GPa. We have noticed that the spectrum at high pressure is quite similar to that observed at ambient pressure below 170 K except for some upshifts due to the compression effects. In particular, a mode located at 1001 cm^{-1} (see the solid square in the inset to Fig. 2) is an exclusive signature of a low temperature phase. The appropriate way of comparing the spectra at high pressure with that recorded at ambient pressure is made by comparing the frequency intercepts ω_0 . We have found that ω_0 for the highest frequency mode for the 0.26–2.2 GPa pressure interval is 999 cm^{-1} , in good agreement with the value measured for the monoclinic phase (1001 cm^{-1}).²⁰ We may therefore conclude that the crystal structure above 0.29 GPa is most likely the same as that of the low temperature phase of $\text{Sc}_2(\text{MoO}_4)_3$. This low temperature structure is ferroelastic, belonging to the space group C_{2h}^5 , and this phase transition is characterized by slight rotations of the MoO_4^{2-} tetrahedra along with a unit cell doubling.¹⁸ The second phase transition is surely connected with significant changes in the crystal structure owing to abrupt frequency changes observed for this phase [see Figs. 1(b) and 2]. It is also interesting to note that usually amorphization in molybdates and tungstates takes place after pressure induced phase transitions.^{7,8,10,11} The study of rare-earth molybdates has also suggested that an orthorhombic to monoclinic phase transition is a precursor for the

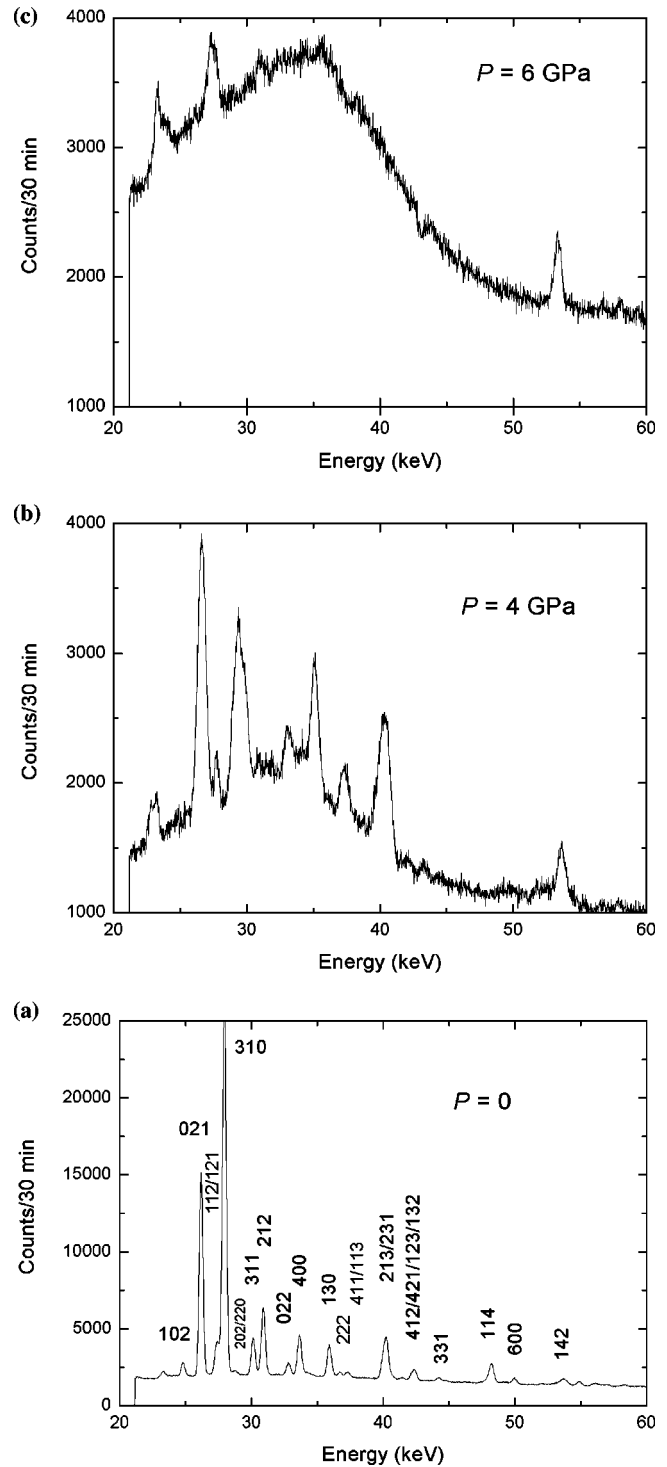


FIG. 3. X-ray diffraction of $\text{Sc}_2(\text{MoO}_4)_3$ recorded at ambient pressure (a), 4.0 GPa (b), and 6.0 GPa (c).

amorphization.¹⁶ This experimental evidence leads us to propose that as a result of the phase transition in the highly flexible framework of the $\text{Sc}_2(\text{MoO}_4)_3$ crystal, the material becomes quite dense and the structure cannot support a further pressure increase because the external pressure brings MoO_4^{2-} units against each other, thus giving rise to a strong repulsion of these units. The competition between the repulsion of the MoO_4^{2-} units and the volume decrease due to external pressure leads the material to lose its long range

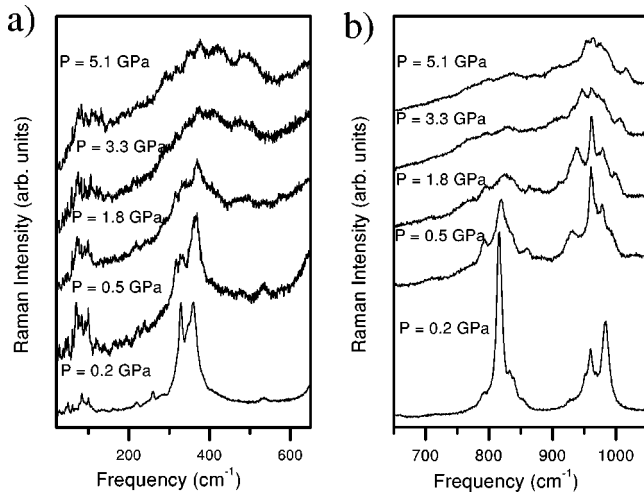


FIG. 4. Raman spectra of $\text{Sc}_2(\text{MoO}_4)_3$ crystals recorded at different pressures during decompression experiments in the (a) low and (b) high frequency regions.

order, thus becoming disordered (amorphous phase), albeit some intact atomic groups should prevail. Our $\text{Sc}_2(\text{MoO}_4)_3$ data show that after amorphization the MoO_4^{2-} tetrahedra units (bands around 350, 800, and 950 cm^{-1}) are present in the material but they are not distributed in a well defined symmetry site. This is confirmed by observing the large line-widths of the bands (50 cm^{-1}) in the Raman spectra of the disordered phase. This result tells us that the amorphous $\text{Sc}_2(\text{MoO}_4)_3$ presents rigid units which are not destroyed during the amorphization process. We now move to analyze the decompression run to get further insights into the amorphization mechanism.

In Fig. 4 we show the Raman spectra for $\text{Sc}_2(\text{MoO}_4)_3$ recorded during a decompression run. Upon releasing pressure from 5.1 GPa the spectrum of the starting orthorhombic phase was recovered, as can be observed in Fig. 4 (see lower trace), thus indicating the reversibility of the processes; however, we have observed some hysteresis in the pressure transition values. The x-ray study shows, however, that upon releasing pressure from 20.0 GPa the amorphous to crystal transition is no longer reversible. These results point out that the amorphous to crystal transition is irreversible and the observed reversibility of this process in the Raman experiment can be attributed to an incomplete transformation (residual crystallinity). The observed gradual, irreversible amorphization and the presence of molybdate tetrahedra in the amorphous phase show that the behavior of $\text{Sc}_2(\text{MoO}_4)_3$ is very similar to the behavior of zirconium tungstate. In the latter case the amorphization was shown to be result of a kinetic hindrance of a phase transition to a new denser hexagonal phase.¹⁴ We then argue that the amorphization process in $\text{Sc}_2(\text{MoO}_4)_3$ is due to steric constraints. The increase of pressure leads to an increase of repulsive forces among oxygen atoms. In order to lower the free energy of the system, the long range order breaks down, thus leading to the appearance of the amorphous phase. As there is no definitive picture, the x-ray measurements^{19,23} in $\text{Sc}_2(\text{WO}_4)_3$ have sug-

gested a phase transition before the amorphization process, which points out that the existence of a phase transition before the amorphization takes place is a general trend for molybdates and tungstates.^{7,8,11,16}

On the basis of the experimental results, we are now in a position to state that on applying pressure the $\text{Sc}_2(\text{MoO}_4)_3$ crystal exhibits a sequence of changing symmetry events. It starts with an orthorhombic structure (D_{2h}^{14}), changes to a low temperature monoclinic phase (C_{2h}^5), changes to a high pressure phase with low symmetry, and finally, an amorphous state takes place for pressures higher than 3.7 GPa. A lowering symmetry path to the amorphous state has been reported for other molybdates and tungstates such as ZrMo_2O_8 , HfW_2O_8 , and ZrW_2O_8 , whose phase transitions are characterized by an abrupt volume decrease and a symmetry lowering sequence as follows: cubic \rightarrow orthorhombic \rightarrow amorphous.⁷⁻¹³ Our data for $\text{Sc}_2(\text{MoO}_4)_3$ also show a similar high pressure behavior when compared with these molybdates and tungstates. This similarity is reasonable since they have quite a close structure with a very flexible framework due to the corner-shared tetrahedra configuration, and also exhibit NTE. The second observed phase transition is surely abrupt. Since it is known that a significant increase in interactions among molecular units results in a decrease of stretching modes frequencies due to increase of the bond lengths,²⁴ the observed frequency decrease of many molybdenum-oxygen stretching modes at the 2.7 GPa phase transition suggests a severe volume decrease at this transition.

IV. CONCLUSIONS

A high pressure Raman study of the $\text{Sc}_2(\text{MoO}_4)_3$ crystal was reported here. We observed that pressure induced two reversible structural transformations and irreversible amorphization in $\text{Sc}_2(\text{MoO}_4)_3$. A clear sequence of symmetry changes in a process that ends up with the loss of translational symmetry, leading to an amorphous state, was observed. Our results point out that pressure does not promote the chemical decomposition in $\text{Sc}_2(\text{MoO}_4)_3$ and the amorphization driven mechanism probably due to a kinetic hindrance of equilibrium phase transition. $\text{Sc}_2(\text{MoO}_4)_3$ should be added to the list of materials with NTE that exhibit amorphization at high pressures. Certainly, the richness of the structural phase transformation in the $\text{Sc}_2(\text{MoO}_4)_3$ crystal observed in a relatively low pressure range will encourage further experimental and theoretical efforts for understanding the amorphization process and its relation with the NTE phenomenon in the large class of molybdates and tungstates compounds with $M_x(\text{XO}_4)_3$ formula.

Note added in proof. After our paper was accepted, a work by Arora *et al.*²⁵ came to our attention.

ACKNOWLEDGMENTS

W.P. and A.G.S.F. acknowledge financial support from the Brazilian agencies CNPq and CAPES (PRODOC Grant No. 22001018), respectively. The authors acknowledge partial support from Brazilian agencies (FUNCAP, CNPq, and

FINEP) and from the Polish Committee for Scientific Research (Grant No. 7TO9A02021). We thank HASYLAB-DESY for permission to use the synchrotron radiation facility. Part of this work was supported by the IHP Contract

HPRI-CT-2001-00140 of the European Commission. Financial support from the Danish Natural Science Research Council through DANSYNC is gratefully acknowledged by L.G., J.S.O., and A.W.

*Author to whom correspondence should be addressed. Email address: agsf@fisica.ufc.br

¹S.M. Sharma and S.K. Sikka, *Prog. Mater. Sci.* **40**, 1 (1996).

²A.K. Arora and T. Sakuntala, *Solid State Commun.* **75**, 855 (1990).

³S.R. Shieh, L.C. Ming, and A. Jayaraman, *J. Phys. Chem. Solids* **57**, 247 (1996).

⁴M.N. Shashikala, N. Chandrabhas, K. Jayaram, and A.K. Sood, *J. Raman Spectrosc.* **24**, 129 (1993).

⁵P. Gillet, J. Badro, B. Varrel, and P.F. McMillan, *Phys. Rev. B* **51**, 11262 (1995).

⁶J.S. Tse, D.D. Klug, J.A. Ripmeester, S. Desgreniers, and K. Lagarec, *Nature (London)* **369**, 724 (1996).

⁷C.A. Perottoni and J.A.H. da Jornada, *Science* **280**, 886 (1998).

⁸T.R. Ravindran, A.K. Arora, and T.A. Mary, *Phys. Rev. Lett.* **84**, 3879 (2000).

⁹T.R. Ravindran, A.K. Arora, and T.A. Mary, *J. Phys.: Condens. Matter* **13**, 11573 (2001).

¹⁰B. Chen, D.V.S. Muthu, Z.X. Liu, A.W. Sleight, and M.B. Kruger, *Phys. Rev. B* **64**, 214111 (2001).

¹¹D.V.S. Muthu *et al.*, *Phys. Rev. B* **65**, 64101 (2002).

¹²T.R. Ravindran, A.K. Arora, and T.A. Mary, *Phys. Rev. B* **67**,

064301 (2003).

¹³H. Liu *et al.*, *J. Phys. Chem. Solids* **64**, 287 (2003).

¹⁴A. Grzechnik, W.A. Crichton, K. Syassen, P. Adler, and M. Mezouar, *Chem. Mater.* **13**, 4255 (2001).

¹⁵A. Jayaraman, S.K. Sharma, and S.Y. Wang, *Pramana* **40**, 357 (1993).

¹⁶V. Dmitriev *et al.*, *J. Phys. Chem. Solids* **64**, 307 (2003).

¹⁷J.S.O. Evans, T.A. Mary, and A.W. Sleight, *J. Solid State Chem.* **133**, 580 (1997).

¹⁸J.S.O. Evans and T.A. Mary, *Int. J. Inorg. Mater.* **2**, 143 (2000).

¹⁹R.A. Secco, H. Liu, N. Imanaka, and G. Adachi, *J. Mater. Sci. Lett.* **20**, 1339 (2001).

²⁰M. Maczka *et al.* (unpublished).

²¹J. Hanuza *et al.*, *J. Solid State Chem.* **105**, 49 (1993).

²²A.K. Tyagi, N.S. Achary, and M.D. Matthews, *J. Alloys Compd.* **339**, 207 (2002).

²³R.A. Secco, H. Liu, N. Imanaka, G. Adachi, and M.D. Rutter, *J. Phys. Chem. Solids* **63**, 425 (2002).

²⁴F.D. Hardcastle and I.E. Wachs, *J. Raman Spectrosc.* **26**, 397 (1995).

²⁵A.K. Arora, R. Nithya, T. Yagi, M. Miyajima, and T.A. Mary, *Solid State Commun.* **129**, 9 (2004).